The Journal of Immunology

In Vivo Maintenance of Human Regulatory T Cells during CD25 Blockade

David J. Huss, Devangi S. Mehta, Akanksha Sharma, Xiaojun You, Katherine A. Riester, James P. Sheridan, Lakshmi S. Amaravadi, Jacob S. Elkins and Jason D. Fontenot

---

References	This article **cites 50 articles**, 17 of which you can access for free at: http://www.jimmunol.org/content/194/1/84.full#ref-list-1

> **Why *The JI*?** Submit online.
>
> • **Rapid Reviews! 30 days*** from submission to initial decision
>
> • **No Triage!** Every submission reviewed by practicing scientists
>
> • **Fast Publication!** 4 weeks from acceptance to publication
>
> **average*

Subscription	Information about subscribing to *The Journal of Immunology* is online at: http://jimmunol.org/subscription
Permissions	Submit copyright permission requests at: http://www.aai.org/About/Publications/JI/copyright.html
Email Alerts	Receive free email-alerts when new articles cite this article. Sign up at: http://jimmunol.org/alerts

AMERICAN ASSOCIATION OF IMMUNOLOGISTS · FOUNDED 1913

In Vivo Maintenance of Human Regulatory T Cells during CD25 Blockade

David J. Huss,* Devangi S. Mehta,* Akanksha Sharma,* Xiaojun You,* Katherine A. Riester,* James P. Sheridan,[†] Lakshmi S. Amaravadi,* Jacob S. Elkins,* and Jason D. Fontenot*

Regulatory T cells (Tregs) mediate immune tolerance to self and depend on IL-2 for homeostasis. Treg deficiency, dysfunction, and instability are implicated in the pathogenesis of numerous autoimmune diseases. There is considerable interest in therapeutic modulation of the IL-2 pathway to treat autoimmunity, facilitate transplantation tolerance, or potentiate tumor immunotherapy. Daclizumab is a humanized mAb that binds the IL-2 receptor α subunit (IL-2Rα or CD25) and prevents IL-2 binding. In this study, we investigated the effect of daclizumab-mediated CD25 blockade on Treg homeostasis in patients with relapsing-remitting multiple sclerosis. We report that daclizumab therapy caused an ~50% decrease in Tregs over a 52-wk period. Remaining FOXP3+ cells retained a demethylated Treg-specific demethylated region in the *FOXP3* promoter, maintained active cell cycling, and had minimal production of IL-2, IFN-γ, and IL-17. In the presence of daclizumab, IL-2 serum concentrations increased and IL-2Rβγ signaling induced STAT5 phosphorylation and sustained FOXP3 expression. Treg declines were not associated with daclizumab-related clinical benefit or cutaneous adverse events. These results demonstrate that Treg phenotype and lineage stability can be maintained in the face of CD25 blockade. *The Journal of Immunology*, 2015, 194: 84–92.

R egulatory T cells (Tregs) are critical mediators of immune tolerance to self. Tregs express high amounts of CD25, the α-chain of the high-affinity IL-2 receptor, and depend on IL-2 for development and maintenance (1, 2). Treg deficiencies owing to genetic mutations in *FOXP3*, the lineage-defining transcription factor, cause a lethal lymphoproliferative autoimmune syndrome in humans and mice (3–6). Treg-mediated suppression is a vital negative regulator of immune-mediated inflammation, and Treg dysfunction is implicated in autoimmune and auto-inflammatory disease (7, 8). Loss of Treg lineage identity and subsequent development of a proinflammatory function by FOXP3+ cells has been proposed as a driver in the development of auto-immune pathologies (9–11).

IL-2 is a pleiotropic cytokine that regulates the biology of multiple immune cell types (12). There is considerable interest in therapeutic modulation of the IL-2 pathway to treat autoimmunity, facilitate transplantation tolerance, or potentiate tumor immuno-therapy. As a growth factor for numerous cell types, including both effector T cells and Tregs, IL-2 has opposing roles in both potentiating and limiting innate and adaptive immunity (13). Thus, the aggregate effect of therapeutic manipulation of IL-2 biology

in vivo, particularly the effect on IL-2–mediated effector T cell response versus Treg-mediated immune tolerance, is not easily predicted but is critical to understand.

Daclizumab, a humanized Ab that binds CD25 and blocks its interaction with IL-2 (14), is currently in clinical development for relapsing-remitting multiple sclerosis (RRMS), a T cell–mediated neuroinflammatory disorder (15–17). Results from a 600-patient, randomized, double-blinded, placebo-controlled trial demonstrated that daclizumab has robust clinical efficacy (18). Thus, in the context of a T cell–mediated autoimmune disease, the dominant effect of targeting CD25 is reduction in autoimmune pathology and therapeutic benefit.

IL-2 signaling is modulated, but not abrogated by Ab-mediated blockade of CD25. CD25 acts to increase the affinity of the heterotrimeric high-affinity IL-2 receptor (CD122, CD132, and CD25) for IL-2, but it does not contribute to the intracellular signal transduction of the receptor (13). Consistent with the pleiotropic biology of IL-2, the mechanism of action of daclizumab extends beyond direct effects on T cells (19). In patients with RRMS, daclizumab therapy causes an increase in circulating CD56^{bright} NK cells (20, 21) and a reduction in circulating lymphoid tissue inducer cells (22). These effects are linked to increased intermediate-affinity receptor-dependent IL-2 signaling, and they have been hypothesized to contribute to the efficacy of daclizumab in RRMS.

Daclizumab therapy reduces the number of circulating Tregs (21, 23). Based on the well-defined role for IL-2 in supporting Treg homeostasis, this effect is not unexpected. However, the qualitative and quantitative impact of CD25 blockade on Treg biology in the context of human autoimmune disease has not been described. The magnitude of the reduction in Tregs and the maintenance of Treg lineage stability among FOXP3+ cells are of particular concern. Recent work has suggested that CD25 blockade on Tregs has the potential to destabilize Treg lineage identity and to generate a population of T cells biased for self-reactivity and production of proinflammatory cytokines (24).

The present study was designed to determine the effect of in vivo CD25 blockade on Treg phenotype and stability and to integrate

these findings into our understanding of the mechanism of action of daclizumab.

Materials and Methods

Patients

PBMCs, serum, and clinical data were collected in the SELECT phase II clinical trial of the daclizumab high-yield process (DAC HYP) (18). This study was conducted in accordance with the Declaration of Helsinki and approved by an institutional review board at each study center. Each patient provided written informed consent at enrollment. Healthy donor blood was obtained from the Biogen Idec blood donor program under a protocol approved by the institutional review board. All donors provided written informed consent. The SELECT trial is registered at ClinicalTrials.gov as identifier NCT00390221.

Whole blood flow cytometry assay for Tregs

Flow cytometric analysis for Tregs was performed at LabCorp Clinical Trials (Mechelen, Belgium) on Vacutainer-collected anticoagulated whole blood specimens, shipped ambient temperature for next-day analysis. Treg percentages, defined as $CD4^+CD127^{low/-}FOXP3^+$ T cells, were determined using anti-CD3 (SK7), anti-CD4 (SK3), and anti-CD127 (M21) from BD Biosciences (San Jose, CA). Anti-FOXP3 (PCH101) and rat IgG2a isotype control Ab (eBR2a) were obtained from eBioscience (San Diego, CA).

Treg-specific demethylated region analysis

Treg-specific demethylated region (TSDR) analysis was performed by Epiontis (Berlin, Germany), as described previously (25). The method was further developed and validated for use with cryopreserved PBMCs. Assay modifications included expanding the standard curve range (30–31,250 copies per reaction), establishing the lower limit of quantification of the assay at 30 copies per reaction, and inclusion of spiked plasmid and reference DNA quality control samples.

Flow cytometry immunophenotyping assay

Treg immunophenotyping was performed on cryopreserved PBMCs. PBMCs were rapidly thawed and washed twice with warm X-VIVO 15 media (Lonza Group, Basel, Switzerland) before staining with anti-CD3 (SK7), anti-CD4 (SK3), anti-CD25 (MA-251), anti-CD31 (M89D3), anti-CD127 (HIL-7R-M21), and anti-CD45RA (HI 100) from BD Biosciences and anti-CD122 (TU27; BioLegend, San Diego, CA). FOXP3 staining was done with a FOXP3-specific buffer system (eBioscience) and anti-FOXP3 (236A/E7; eBioscience). For detection of intracellular cytokine secretion, cells were activated with 50 ng/ml PMA and 500 ng/ml ionomycin in the presence of GolgiStop Protein Transport Inhibitor (BD Biosciences) for 3.5 h. After staining for cell surface molecules, cells were fixed and permeabilized with an FOXP3-specific buffer system (eBioscience) and stained with anti-FOXP3 (236A/E7; eBioscience), anti–IL-17A (eBio64DEC17; eBioscience), anti–IL-2

(MQ1-17H12; BD Biosciences), anti–IFN-γ (B27; BD Biosciences), anti–CTLA-4 (BNI3; BD Biosciences), and anti–Ki-67 (B56; BD Biosciences). At least 300,000 events were acquired on a BD LSR II (BD Biosciences) flow cytometer for analysis using FlowJo software (Tree Star, Ashland, OR).

Serum IL-2 measurement

An Imperacer immuno-PCR–based method for ultrasensitive quantification of human IL-2 in serum in the range of 1–1000 pg/ml was developed and validated (performed by Chimera Biotec, Dortmund, Germany). Detection of serum IL-2 was performed in a sandwich immunoassay format, using surface immobilized anti–IL-2 capture Ab in combination with anti–IL-2 Ab-DNA detection conjugate (26). Assay validation included assessment of standard curve performance, accuracy and precision, dilutional linearity, selectivity, and sample stability. If the sample concentration result value was less than the lower limit of quantification (<1 pg/ml), then a value of 0.5 pg/ml was assigned for the purpose of data analysis.

STAT5 phosphorylation assay

Cryopreserved PBMCs were rapidly thawed and rested for 2 h at 37°C in X-VIVO 10 media (Lonza Group). PBMCs were then left untreated or treated with DAC HYP (15 μg/m) or anti-CD122 (5 μg/m; clone TU27; BioLegend), or both, for 30 min at 37°C before being stimulated with recombinant human IL-2 (R&D Systems, Minneapolis, MN) for 20 min at 37°C. Cells were then fixed with Cytofix buffer (BD Biosciences) for 10 min at 37°C and permeabilized with PhosFlow Buffer III (BD Biosciences) for 30 min on ice. Cells were then stained with anti-CD3 (SK7), anti-CD4 (SK3), anti-FOXP3 (259D/C7), anti-CD45RA (HI 100), anti-CD25 (M-A251), anti-CD8 (RPA-T8), and anti-pSTAT5 (pY694) obtained from BD Biosciences for 45 min at room temperature. At least 100,000 events were acquired on a BD LSR II for analysis using FlowJo software.

Statistical analysis

For comparison of two groups, Student independent sample t test was used for analysis of independent groups, and paired t test was used for analysis of repeated measurements within identical groups of patients. When data were not normally distributed, a nonparametric test (Mann–Whitney) was used. Statistical analysis of Treg dynamics in the entire SELECT cohort was performed using a negative binomial model with specific adjustments (defined in Table I), or a Wilcoxon rank-sum test (defined in Table II). Treatment response was defined by the ratio of observed to expected new or newly enlarging T2 lesions, where the expected number of new or newly enlarging T2 lesions was estimated from a negative binomial regression model with covariates for baseline number of T2 lesions, treatment group, baseline T2 volume, baseline Expanded Disability Status Scale score, number of relapses in the previous year, and number of baseline gadolinium-enhancing lesions. In all statistical analyses, a p value < 0.05 was considered significant.

Table I. Treg dynamics do not associate with treatment response in DAC HYP–treated patients

Treatment Responder Status	Treg Measures	n	Mean	Median	SD	Min	Max	p^a
Quartile 4 response (active MS)	Treg counts[b] at baseline	81	13.18	10.25	11.71	0.53	77.03	0.241
	Treg counts at week 24	79	4.67	3.91	3.30	0.47	17.98	0.836
	Treg counts at week 52	71	5.15	4.10	3.39	0.00	16.36	0.733
	Percentage change of Treg counts from baseline to week 24	77	−0.39	−0.63	0.75	−0.96	3.80	0.412
	Percentage change of Treg counts from baseline to week 52	68	−0.33	−0.50	0.74	−1.00	3.81	0.124
Quartile 1 response (controlled MS)	Treg counts at baseline	84	14.40	11.54	10.27	0.55	56.59	–
	Treg counts at week 24	79	5.05	3.68	4.41	0.46	19.51	–
	Treg counts at week 52	80	5.88	4.48	5.02	0.33	29.13	–
	Percentage change of Treg counts from baseline to week 24	74	−0.46	−0.69	0.75	−0.98	4.10	–
	Percentage change of Treg counts from baseline to week 52	74	−0.23	−0.68	1.85	−0.96	14.60	–

[a]The p values are from Wilcoxon rank-sum test.
[b]Counts represent cells/mm^3 of whole blood.
max, maximum; min, minimum; MS, multiple sclerosis.

Table II. Treg dynamics do not associate with CUT-AEs in DAC HYP–treated patients

AE Status	Treg Measures	n	Mean	Median	SD	Min	Max	p^a
Diffuse rash CUT-AE	Treg counts[b] at baseline	11	17.24	16.91	14.08	4.98	48.62	0.55
	Treg counts at week 24	11	5.41	3.62	5.54	0.76	19.51	0.78
	Treg counts at week 52	11	6.92	6.19	3.79	1.22	14.03	0.10
	Percentage change of Treg counts from baseline to week 24	11	−0.41	−0.70	0.99	−0.98	2.53	0.38
	Percentage change of Treg counts from baseline to week 52	11	−0.26	−0.42	0.71	−0.97	1.44	0.40
Non-AE	Treg counts at baseline	315	13.38	11.52	9.20	0.53	77.03	–
	Treg counts at week 24	295	4.96	3.96	3.67	0.00	22.64	–
	Treg counts at week 52	282	5.36	4.23	3.91	0.00	29.13	–
	Percentage change of Treg counts from baseline to week 24	277	−0.48	−0.63	0.57	−1.00	4.10	–
	Percentage change of Treg counts from baseline to week 52	262	−0.38	−0.61	1.11	−1.00	14.60	–

[a]The p values are from Wilcoxon rank-sum test.
[b]Counts represent cells/mm^3 of whole blood.
AE, adverse event; CUT-AE, cutaneous adverse event; max, maximum; min, minimum; MS, multiple sclerosis; non-AE, patients who did not experience an adverse event.

Results

CD4$^+$CD127$^{low/-}$FOXP3$^+$ cells decline in DAC HYP–treated patients with RRMS

DAC HYP, a version of daclizumab developed for s.c. administration, was recently studied in the SELECT trial (18). The effect of DAC HYP on CD4$^+$CD127$^{low/-}$FOXP3$^+$ cell numbers was determined by flow cytometric analysis of patients' blood at baseline and at multiple time points after treatment. Placebo-treated patients had stable numbers of CD4$^+$CD127$^{low/-}$FOXP3$^+$ cells during the 52-wk study period, whereas CD4$^+$CD127$^{low/-}$FOXP3$^+$ cells in DAC HYP–treated patients declined by ~50% from baseline to week 8 and then stabilized at subsequent time points in the 52-wk study period (Fig. 1).

DAC HYP differentially affects Treg subsets and Treg-associated markers

We sought to address whether the CD4$^+$CD127$^{low/-}$FOXP3$^+$ cells that remained in DAC HYP–treated patients retained the characteristics of bona fide Tregs. Flow cytometry was used to identify CD45RA$^+$CD25$^+$FOXP3$^+$ resting Tregs (rTregs) and CD45RA$^-$CD25^{++}FOXP3^{++} activated Tregs (aTregs) in PBMCs from a cohort of SELECT study patients (placebo, n = 34; DAC HYP, n = 75) (27). For comparison, canonical Tregs, as defined by CD4$^+$CD127$^{low/-}$FOXP3$^+$, were included in all analyses. In placebo-treated patients with RRMS, both aTregs and rTregs remained stable from baseline to week 24; however, DAC HYP therapy resulted in a reduction in each Treg subset measured (Fig. 2A). When the magnitude of change was analyzed, aTregs (45.8% decline) were more significantly affected when compared with rTregs (29.7% decline; p < 0.05). On both aTregs and rTregs, CD25 expression significantly decreased with DAC HYP therapy, whereas CD122 expression remained stable (Fig. 2B, 2C). Despite the substantial decrease in CD25 expression, FOXP3 expression was only modestly decreased in each Treg subset (mean change from baseline of < 10%; Fig. 2D).

Tregs that remain in DAC HYP–treated patients maintain a stable phenotype

Given the decline in CD4$^+$CD127$^{low/-}$FOXP3$^+$ cells and the role for IL-2 in maintaining Tregs, we next analyzed the phenotype of the remaining FOXP3$^+$ cells for characteristics of bona fide Tregs. We assessed Ki-67 expression as a marker for actively cycling cells in the rTreg and aTreg populations at baseline and week 24 in DAC HYP– and placebo-treated patients with RRMS. To contrast regulatory and effector T cell phenotype, CD4$^+$ memory T cells

(Tmem; CD4$^+$CD45RA$^-$FOXP3$^-$) were included in the analysis. DAC HYP therapy did not affect the percentage of Ki-67$^+$ rTregs and aTregs (Fig. 3A). We next analyzed rTreg and aTreg production of proinflammatory cytokines ex vivo. The production of IL-2, IFN-γ, and IL-17 remained low in Tregs, indicating that Tregs were not acquiring an effector T cell phenotype (Fig. 3B–3D). We also assessed the expression of CTLA4 and ICOS molecule. The percentage of CTLA4$^+$ cells within the rTreg and aTreg gates modestly decreased (Fig. 3E), whereas ICOS$^+$ cell percentages remained consistent (Fig. 3F). By these metrics, Tregs present during Ab-mediated CD25 blockade are phenotypically similar to Tregs present before treatment or in untreated patients with RRMS.

Tregs that remain in DAC HYP–treated patients maintain TSDR demethylation

Treg stability is epigenetically regulated at the FOXP3 locus (28–30). Lineage-committed human Tregs can be distinguished from transient FOXP3-expressing effector T cells by the presence of a demethylated TSDR (27, 31, 32). Given the importance of IL-2 in driving FOXP3 expression and the modest decrease we observed in FOXP3 expression in Tregs during DAC HYP therapy, we sought to determine whether CD25 blockade effected TSDR methylation status. To perform this analysis, we measured epigenetically committed, stable Tregs using a quantitative PCR assay that enumerates Tregs based on the presence of a demethylated TSDR, termed TSDR$^+$ Tregs (25, 33). In addition, total cells and CD3$^+$ T cells were simultaneously quantified in the
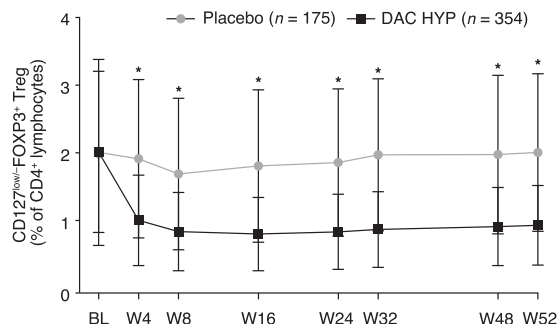
FIGURE 1.   CD4$^+$CD127$^{low/-}$FOXP3$^+$ cells decline in DAC HYP–treated patients. Flow cytometry was performed on anticoagulated whole blood samples to identify CD127$^{low/-}$FOXP3$^+$ Tregs in patients with RRMS randomized to placebo (n = 175) or DAC HYP (n = 354). Gating was based on isotype control staining. Data are shown as means ± SD. *p < 0.0001. BL, baseline; W, week.
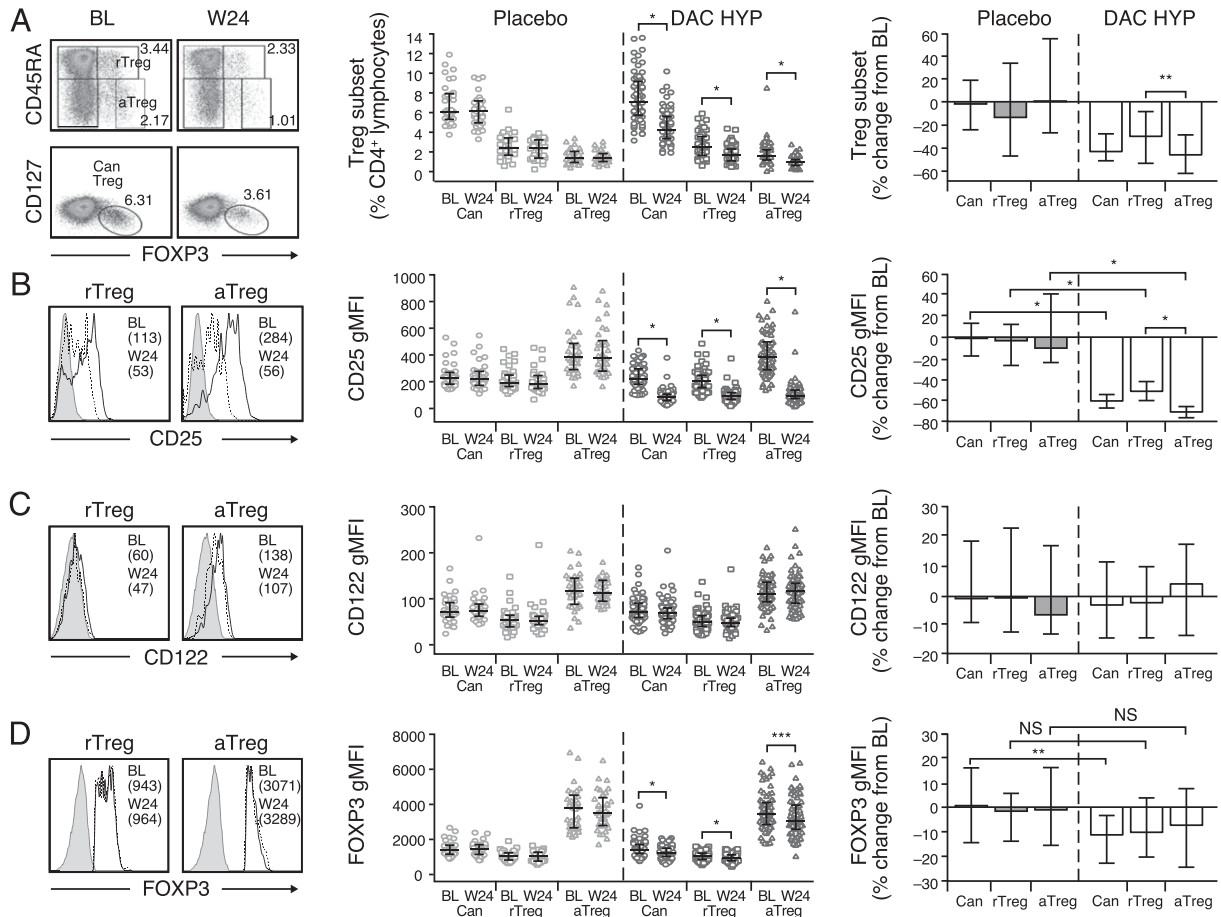
FIGURE 2. DAC HYP differentially affects Treg subsets and Treg-associated markers. Flow cytometry was used to identify can Treg (CD127$^{low/-}$FOXP3$^+$), rTreg (CD45RA$^+$FOXP3$^+$), and aTreg (CD45RA$^-$FOXP3^{++}) cell subsets in patients with RRMS treated with DAC HYP ($n = 75$) or placebo ($n = 34$). Analysis was conducted at BL and W24. (**A**) Representative dot plots within the CD3$^+$CD4$^+$ lymphocyte gate demonstrate Treg gating strategy. Scatter plots demonstrate percentage of each Treg population within the CD3$^+$CD4$^+$ lymphocyte gate at BL and W24. Bar graphs demonstrate percentage change of each Treg population from BL to W24. (**B–D**) Representative histograms gated on rTreg and aTreg subsets with the gMFI at BL (solid line) and W24 (dotted line). Scatter plots demonstrate gMFI of each Treg population at BL and W24. Bar graphs demonstrate percentage change in gMFI from BL to W24. Excluding panel (A), data are shown as medians ± interquartile range. *$p < 0.0001$, **$p < 0.05$, ***$p < 0.001$. aTreg, activated regulatory T cell; BL, baseline; can, canonical; DAC HYP, daclizumab high-yield process; gMFI, geometric mean fluorescent intensity; W, week.

sample using epigenetic analysis of the *GAPDH* and *CD3D/CD3G* loci, respectively, and TSDR$^+$ Tregs were calculated as a percentage of total PBMCs or as a percentage of total CD3$^+$ T cells.

In placebo-treated patients, TSDR$^+$ Tregs were stable from baseline through week 52 (Fig. 4A). In patients treated with DAC HYP, there was a reduction in TSDR$^+$ Tregs from baseline to weeks 24 and 52 (Fig. 4A), consistent with the decline in Tregs observed in flow cytometric analyses. To demonstrate further that the Tregs that remain during DAC HYP therapy maintain TSDR demethylation, we compared the Treg flow cytometry analysis to TSDR$^+$ Tregs. Tregs identified by flow cytometry and TSDR analysis showed a statistically significant positive correlation in both placebo- ($r^2 = 0.612$; $p < 0.0001$) and DAC HYP–treated ($r^2 = 0.696$; $p < 0.0001$) patients (Fig. 4B). These results suggested that although Treg numbers are reduced in DAC HYP–treated patients, remaining Tregs maintain a demethylated TSDR, indicating that a stable and lineage-committed Treg population is maintained during CD25 blockade.

Intermediate-affinity IL-2Rβγ signaling induces pSTAT5 and FOXP3 expression in Tregs

DAC HYP inhibits high-affinity CD25-dependent IL-2 signaling while leaving intact intermediate-affinity IL-2Rβγ signaling. To identify potential CD25-independent Treg survival mechanisms,

we assessed intermediate-affinity IL-2 receptor expression on regulatory and conventional CD4$^+$ T cell subsets from PBMCs of untreated patients with RRMS. CD25 and CD122 (IL-2Rβ) were more highly expressed on aTregs compared with rTregs (Fig. 5A, 5B). CD4$^+$ naive and memory T cells expressed lower levels of CD25 and CD122 than either rTregs or aTregs (Fig. 5A, 5B).

We then sought to determine how these differences in receptor expression influenced pSTAT5 in response to IL-2 stimulation. PBMCs from healthy donors were stimulated with IL-2 and pSTAT5 was measured using flow cytometry. To distinguish between high- and intermediate-affinity IL-2R signaling, DAC HYP was used in vitro to block IL-2 binding to CD25. Representative histograms are shown in Fig. 5C. In the absence of DAC HYP, CD25 expression level determined the magnitude of pSTAT5 in response to IL-2 stimulation (Fig. 5C, 5D). When CD25 signaling was blocked, CD122 expression level determined the magnitude of pSTAT5. In the presence of an Ab that blocks IL-2 binding to the IL-2Rβ-chain (α-CD122 Ab), IL-2–mediated pSTAT5 was completely inhibited. Thus, intermediate-affinity IL-2 receptor signaling is preserved in the presence of DAC HYP.

IL-2–induced pSTAT5 engages STAT5-mediated FOXP3 expression (34, 35). To determine whether IL-2Rβγ–mediated pSTAT5 led to downstream FOXP3 expression, PBMCs from
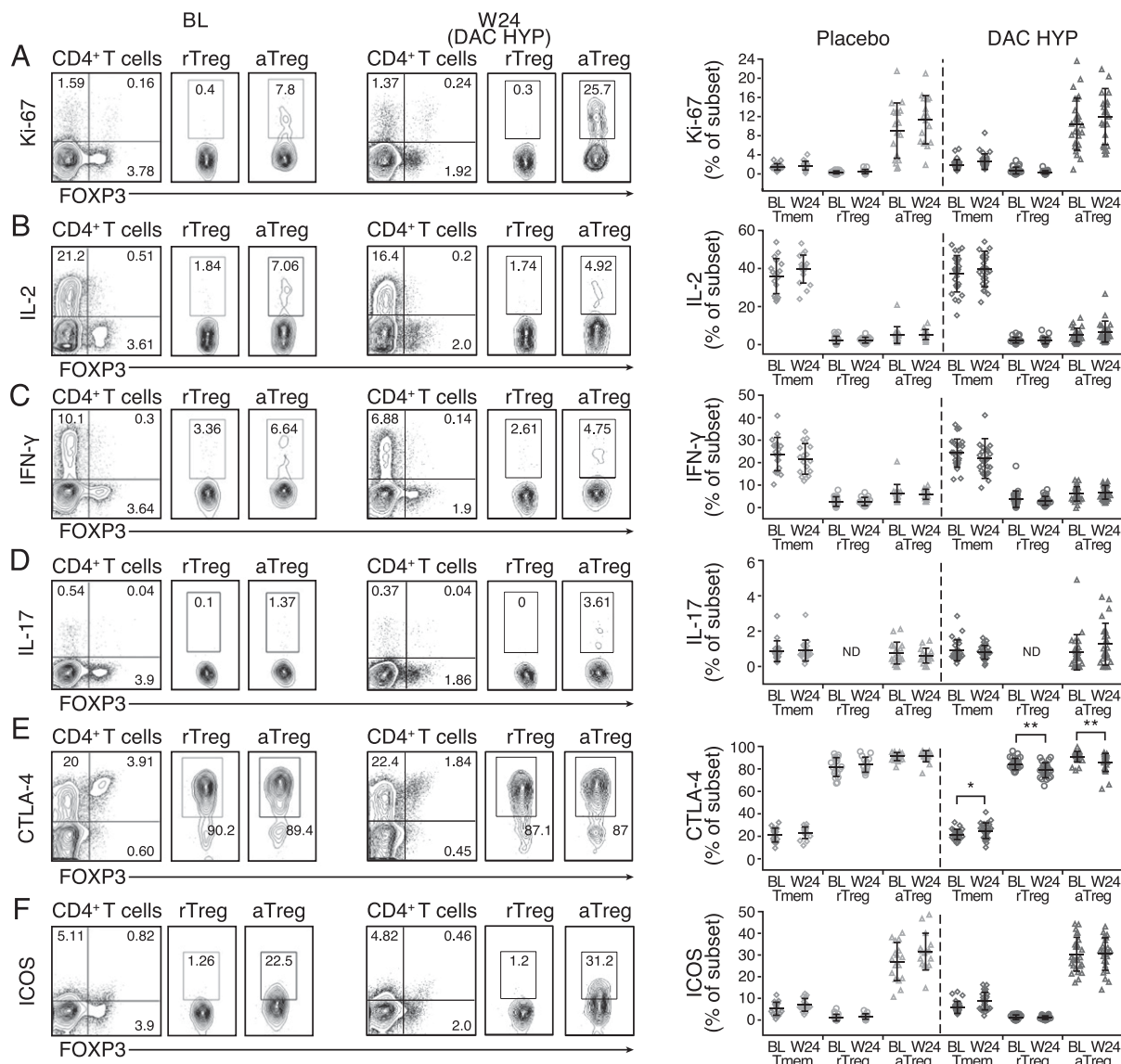
FIGURE 3. Tregs that remain in DAC HYP–treated patients maintain a stable phenotype. PBMCs from DAC HYP– ($n = 27$) and placebo-treated ($n = 18$) patients with RRMS at BL and W24 were stimulated ex vivo with PMA and ionomycin in the presence of GolgiStop. Representative dot plots are gated on total CD4^{+} T cells, rTregs (CD45RA^{+}FOXP3^{+}), or aTregs (CD45RA^{–}FOXP3^{++}) as indicated. All gates are based on isotype control staining (**C**, **D**, and **F**) or fluorescence minus one control staining (**A**, **B**, and **E**). Scatter plots demonstrate the percentage of cells expressing each analyte within the CD4^{+} Tmem cell population, rTreg, and aTreg subsets. Statistical analysis compared each analyte on each cell population at BL and W24. Data are shown as means ± SD. *$p < 0.05$, **$p < 0.0001$. BL, baseline; ND, not detectable; W, week.

healthy donors were stimulated with IL-2 for 24 h, and FOXP3 protein expression in aTregs and rTregs was measured by flow cytometry. IL-2 stimulation alone led to 2.9-fold and 2.2-fold inductions of FOXP3 in aTregs and rTregs, respectively (Fig. 5E, 5F). IL-2–mediated FOXP3 expression was reduced in the presence of DAC HYP, but significant FOXP3 induction still occurred when compared with unstimulated Tregs. α-CD122 Ab inhibited IL-2–mediated FOXP3 expression completely (no difference when compared with baseline levels). Thus, IL-2Rβγ signaling can induce pSTAT5 and subsequent FOXP3 expression during Ab-mediated blockade of CD25.

DAC HYP therapy increases serum IL-2 levels

We hypothesized that DAC HYP therapy can increase IL-2 bioavailability by antagonizing the negative feedback loop that limits IL-2 production by conventional CD4^{+} T cells or by limiting CD25-mediated IL-2 consumption. IL-2 serum concentration was measured in DAC HYP– and placebo-treated patients at baseline,

week 24, and week 52. CD25 blockade caused a significant and sustained ~2-fold increase in serum IL-2 at weeks 24 and 52 compared with baseline (Fig. 6). Of note, at baseline, 31% of DAC HYP–treated patients had serum IL-2 levels below the limit of detection, whereas by week 52, only 3% remained below the limit of detection. Serum IL-2 levels were stable from baseline to week 24 in placebo-treated patients. These results suggest that intermediate-affinity IL-2Rβγ signaling is actually enhanced in DAC HYP–treated patients because of enhanced IL-2 availability.

Intermediate-affinity IL-2Rβγ signaling induces pSTAT5 in Tregs from DAC HYP–treated patients

DAC HYP therapy alters the cellular composition of PBMCs (i.e., decreased Tregs and increased CD56^{bright} NK cells), likely altering competition for IL-2. To extend the observations in healthy donor PBMCs and to determine whether Tregs from DAC HYP–treated patients respond to IL-2 via IL-2Rβγ signaling, we performed ex vivo IL-2 stimulations of PBMCs from DAC HYP–
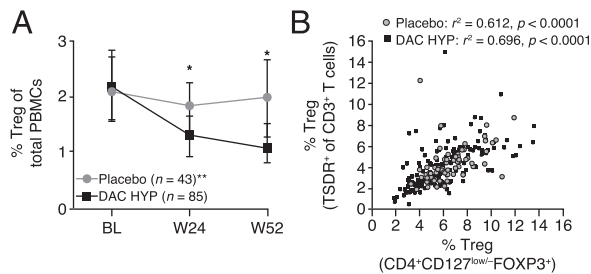
FIGURE 4. Tregs that remain in DAC HYP–treated patients maintain TSDR demethylation. TSDR demethylation analysis was performed on PBMCs from DAC HYP– ($n = 85$) and placebo-treated ($n = 43$) patients with RRMS using bisulfite-converted genomic DNA in a quantified PCR assay. (**A**) TSDR$^+$ Tregs as a percentage of total PBMCs at BL, W24, and W52 in placebo- and DAC HYP–treated patients. Data are shown as medians $\pm$ interquartile range. (**B**) Correlation of Tregs identified by TSDR$^+$ analysis or flow cytometry at W24 for placebo (gray circles) or DAC HYP (black squares) treatment groups. For each method, data are shown as a percentage of CD3$^+$ cells. r^2 values were derived using Spearman correlation. **$n = 19$ for placebo at W24. *$p < 0.0001$. BL, baseline; W, week.

treated patients and compared the pSTAT5 at baseline to week 24. CD25 receptor saturation with DAC HYP is maintained through the cryopreservation and thawing process (data not shown), making addition of exogenous DAC HYP to these ex vivo stimulations unnecessary. All CD4$^+$ T cell subsets analyzed in week 24 PBMCs stimulated with IL-2 had reduced pSTAT5 (Fig. 7A, 7B). Addition of an α-CD122–blocking Ab resulted in near complete inhibition of pSTAT5. Notably, naive and memory T cells have lower expression of the IL-2Rβ-chain (Fig. 5B) and subsequently had little pSTAT5 at week 24 (Fig. 7B).

Tregs maintain a competitive advantage for IL-2 during CD25 blockade

Tregs have a competitive advantage for IL-2 over conventional CD4$^+$ T cells because of their high CD25 expression. Tregs also express higher levels of the IL-2Rβ chain than conventional CD4$^+$ T cells do (Fig. 5B). We examined whether Tregs maintain a competitive advantage over conventional T cells for IL-2 access through intermediate-affinity IL-2R$\beta\gamma$ signaling during CD25 blockade. PBMCs from DAC HYP–treated patients with RRMS at baseline and week 24 were stimulated ex vivo with IL-2. pSTAT5 was measured in all CD4$^+$ T cell subsets using flow cytometry. In both baseline and week 24 samples, rTregs and aTregs had more pSTAT5 when compared with naive and memory CD4$^+$ T cells (Fig. 7C). rTregs maintained a 1.6–1.9-fold advantage for IL-2 over naive CD4$^+$ T cells, whereas aTregs maintained a 2.1–2.4-fold advantage for IL-2 over memory CD4$^+$ T cells. This result suggests that in DAC HYP–treated patients, Tregs maintain a competitive advantage for IL-2 over conventional T cells.

Treg changes do not predict DAC HYP therapy response or cutaneous adverse events

Treg dysfunction is implicated in RRMS pathogenesis (36–43). Notably, DAC HYP has demonstrated robust clinical efficacy despite an overall ~50% reduction in circulating Tregs. We investigated whether individual variation in changes in Treg numbers was associated with DAC HYP therapy response. For this analysis, we compared top-quartile responders (controlled multiple sclerosis) to the bottom-quartile responders (active multiple sclerosis) as described in detail in *Materials and Methods*. Comparisons of Treg counts (Tregs/mm^3 of whole blood) at baseline revealed no significant difference between high- and low-responder quartiles

(Table I). Because DAC HYP therapy causes a decline in Tregs, we also analyzed Treg counts at weeks 24 and 52 and the percentage change from baseline to weeks 24 and 52. These parameters did not associate with treatment response (Table I).

Approximately 20% of patients treated with DAC HYP in the SELECT trial experienced skin rashes defined as cutaneous adverse events (CUT-AEs), compared with 13% in the placebo group (18). Based on case review from an independent dermatologist who was blinded to information about Treg analyses, we identified 11 patients in SELECT who experienced a pattern of diffuse rash that was consistent with a potential role for DAC HYP. An analysis of Tregs in these 11 CUT-AE patients and in patients who did not experience an adverse event showed no association with Treg measurements at baseline, week 24, week 52, or the change in Tregs from baseline to weeks 24 or 52 (Table II).

Discussion

The goal of this study was to understand the in vivo effects of CD25 blockade on human Treg phenotype and lineage stability. Results showed that over a 52-wk period, CD4$^+$CD127$^{low/–}$FOXP3$^+$ cell numbers declined by ~50% in DAC HYP–treated patients with RRMS. FOXP3$^+$ cells that remained maintained the phenotypic and epigenetic properties of Tregs and did not acquire effector T cell characteristics. These data support the important finding that human Treg phenotype and lineage stability can be sustained through CD25-independent signaling mechanisms.

Loss of Treg lineage identity and development of proinflammatory functions by Tregs has been proposed as a driver in the development of autoimmune pathologies. In mice, the majority of Tregs are stable during immune homeostasis; however, in certain inflammatory conditions Treg instability is observed (9, 11, 44–46). The role of the IL-2 axis in this process is still unclear. NOD mice, which have a genetic deficiency in IL-2 signaling, have decreased *FOXP3* expression and increased propensity for Treg instability (9). Rubtsov et al. (45) demonstrated that IL-2 deprivation led to a decrease in total FOXP3$^+$ cells and a modest decrease in FOXP3 protein expression at the single-cell level, but it did not cause conversion of Tregs to an effector T cell phenotype (45). This result is strikingly similar to our observations in patients with RRMS treated with DAC HYP, wherein both rTregs and aTregs decline, FOXP3 expression is only modestly decreased (<10%), TSDR demethylation is maintained, and there is no increase in IL-2, IFN-γ, or IL-17 production. In addition, the result that Tregs in DAC HYP–treated patients maintained Ki-67 expression is of significance, because Treg self-renewal has been shown to be a major mechanism that maintains the Treg population (45). One possible caveat to our analysis would be if some Tregs completely lost expression of FOXP3 during CD25 blockade. Such cells would not be traceable and thus cannot be analyzed; however, our analysis of effector CD4$^+$ T cell populations did not reveal an increase in proinflammatory cytokine-producing cells.

Regarding the functional status of the Tregs that remain in DAC HYP–treated patients, DAC HYP therapy results in a significant decrease in CD25 expression (Fig. 2B) (47), thus preventing the identification and purification of Tregs to perform classical in vitro suppression assays. Despite this technical limitation, our analysis demonstrating that Treg cytokine production, Ki-67 expression, and TSDR status are stable between baseline and week 24 strongly suggests that Tregs maintain their functional identity. Although we cannot rule out subtle changes to Treg-suppressive function in DAC HYP–treated patients, TSDR$^+$ Tregs have consistently been demonstrated to represent functionally suppressive Tregs (27, 31, 32).

Given the stabilization of Treg numbers after 8 wk of DAC HYP therapy, we hypothesized that a CD25-independent signaling
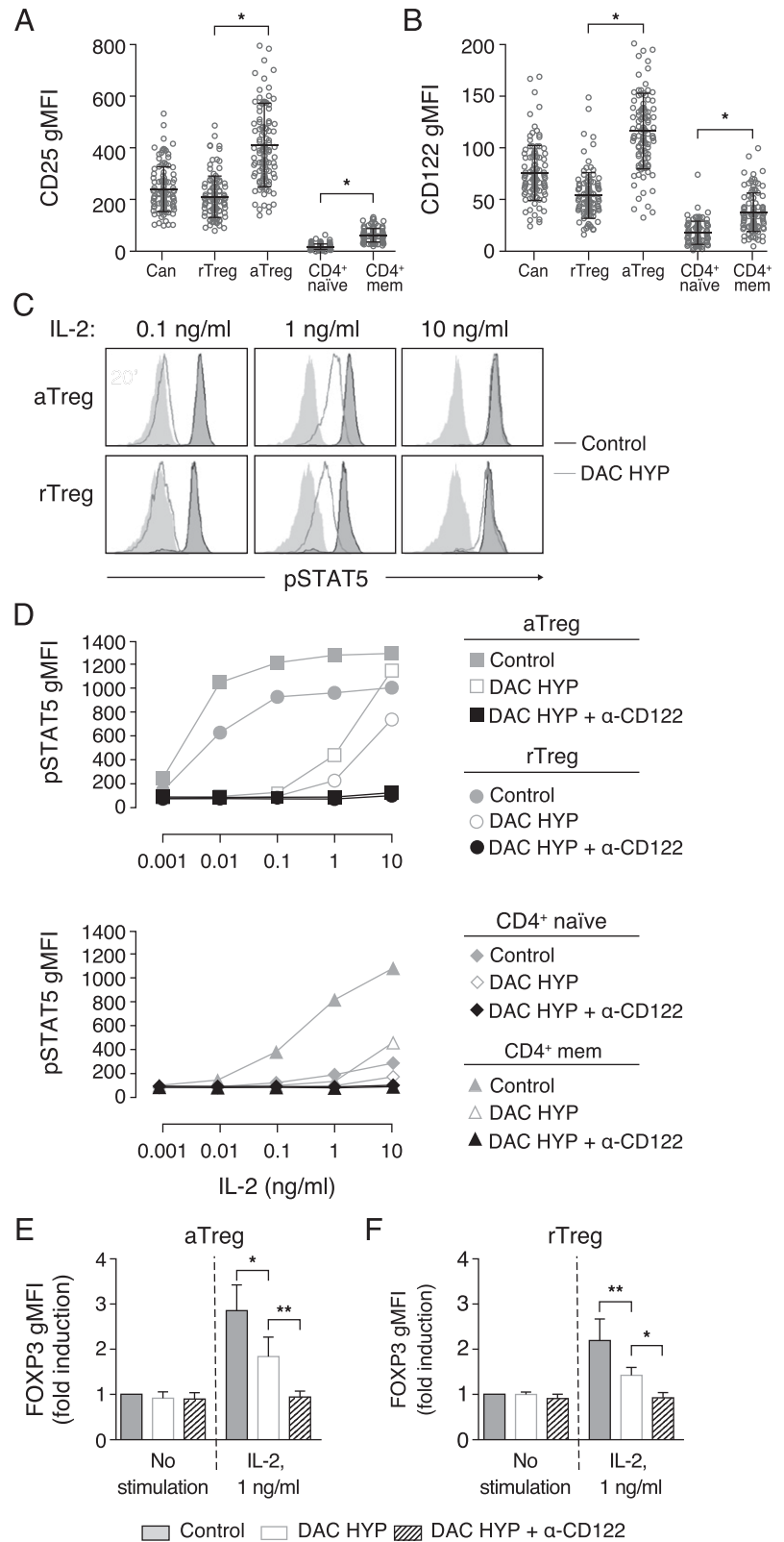
FIGURE 5. Expression of the IL-2R components drives pSTAT5 kinetics and FOXP3 expression. (**A** and **B**) Flow cytometry was performed on PBMCs from untreated patients with RRMS ($n = 109$) to identify Treg subsets and CD4+ naive and Tmem cells. gMFI was quantified for (A) CD25 or (B) CD122 on each cell population. (**C** and **D**) Healthy donor PBMCs were freshly isolated from whole blood and stimulated with IL-2 in the presence of DAC HYP or DAC HYP plus α-CD122. pSTAT5 was measured by flow cytometry using PhosFlow. Data are representative of six independent experiments. (**E** and **F**) Healthy donor PBMCs were freshly isolated from whole blood and stimulated with IL-2 for 24 h. Flow cytometry was used to identify FOXP3 expression in (E) aTregs and (F) rTregs. Fold change was calculated using FOXP3 gMFI and normalizing to the no-stimulation condition for each sample. Data are shown as mean ± SD. *$p < 0.0001$, **$p < 0.001$. can, canonical; gMFI, geometric mean fluorescent intensity; mem, memory.

pathway sustained the remaining Tregs. Our results showed that IL-2 signaling through the intermediate-affinity IL-2Rβγ is preserved in Tregs during CD25 blockade, and it can induce pSTAT5 and subsequent FOXP3 expression. Consistent with the expected effect of daclizumab on effector T cells (14), the pSTAT5 data also showed a reduction in the ability of naive and memory-conventional CD4+ T cells to respond to IL-2. These results suggested that daclizumab raises the threshold for IL-2 signaling in all T cell populations, yet Tregs maintain a competitive advantage for IL-2 over effector T cells.

Consistent with in vitro studies demonstrating that IL-2 signaling inhibits its own production (48) and the potential for reduced IL-2 consumption during CD25 blockade, these findings demonstrated that DAC HYP therapy resulted in increased serum IL-2 levels.
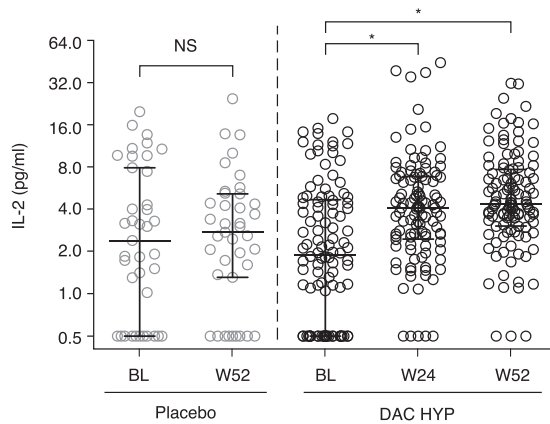
FIGURE 6. Serum IL-2 levels increase in DAC HYP–treated patients. Serum IL-2 levels were measured using a validated Imperacer immuno-PCR in placebo-treated patients ($n = 45$) at BL and W52 and in DAC HYP–treated patients ($n = 130$) at BL and W24 and W52. Data are shown as median $\pm$ interquartile range. *$p < 0.0001$. BL, baseline; W, week.

This increase in serum IL-2 likely enhances IL-2Rβγ signaling over homeostatic conditions in the absence of CD25 blockade and contributes to Treg maintenance. It previously has been hypothesized, but not demonstrated, that a daclizumab-mediated increase in circulating IL-2 also can contribute to observed increases in CD56bright NK cell numbers in daclizumab-treated patients (21). Our data provide in vivo confirmation that CD25 blockade increases circulating IL-2 levels in humans, which suggests that this effect contributes to the expansion of CD56bright NK cells and the maintenance of reduced but stable numbers of Tregs.

The exact mechanism by which DAC HYP reduces Treg numbers is unclear and is difficult to determine experimentally in vivo. In vitro, DAC HYP does not cause complement dependent cytotoxicity and causes minimal Ab-dependent cellular cytotoxicity (Ref. 24 and data not shown). Because IL-2 signaling promotes Treg survival, it is difficult to define whether DAC HYP reduces Treg numbers through Ab-dependent cellular cytotoxicity, by blocking the IL-2 survival signal, or a combination of these two mechanisms.

The cellular and molecular factors that trigger the adverse events observed in the SELECT trial remain unclear. Our results demonstrate that Treg numbers and the change in Treg numbers do not associate with cutaneous adverse events. Analysis of other immune cell changes in DAC HYP–treated patients, particularly the expansion of CD56bright NK cells, also did not reveal an association with adverse events (data not shown). The origin of adverse events in DAC HYP–treated patients may be more complex than a change in a single immune cell population. This area of investigation is active.

In considering the role of Tregs in human autoimmune disease, the robust efficacy of daclizumab in patients with RRMS despite the significant decline in Tregs is notable, particularly given the numerous reports suggesting that Treg dysfunction contributes to RRMS pathogenesis (36–39, 41–43). However, the effect of daclizumab on Tregs does not occur in isolation. Reduction in Tregs must be considered in the context of the effects of CD25 blockade on effector T cells. In addition, daclizumab has profound effects on cells of the innate immune system, including an expansion of CD56bright NK cells (20, 21, 49, 50). It has been proposed that CD56bright NK cells play an immunoregulatory role through a granzyme K–mediated targeting of activated effector T cells (49). Thus, expansion of CD56bright NK cells might contribute to the efficacy of daclizumab and the maintenance of immune tolerance by keeping autoreactive T cells in check.
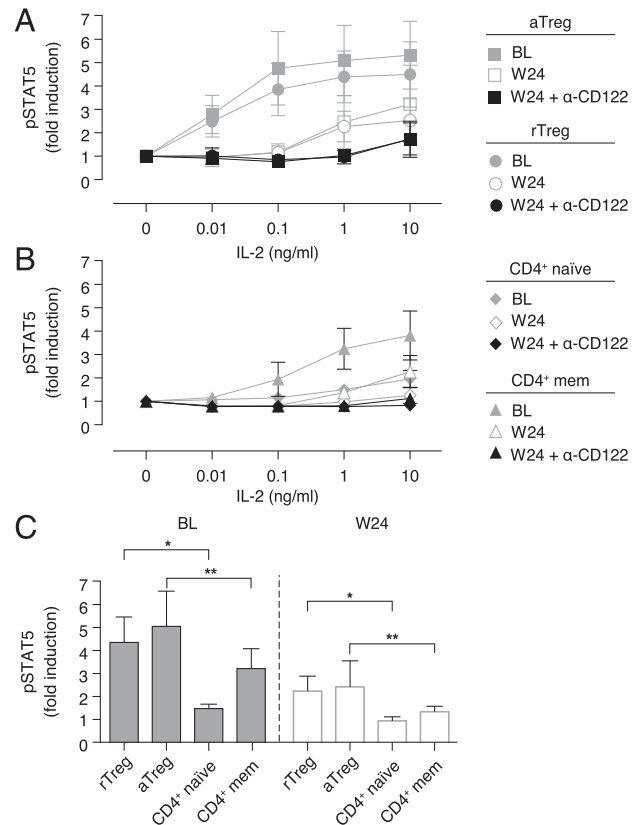
FIGURE 7. During CD25 blockade, Tregs maintain a competitive advantage for IL-2 over effector T cells via IL-2Rβγ signaling. PBMCs from DAC HYP–treated patients with RRMS ($n = 6$) at BL and W24 were stimulated ex vivo with IL-2 for 20 min. Flow cytometry was then used to measure pSTAT5 in (**A**) aTreg and rTreg and (**B**) naïve and mem CD4+ T cell populations. (**C**) Data from (A and B, 1 ng/ml condition) displayed as a direct Treg-to-effector T cell comparison. Fold change was calculated using pSTAT5 geometric mean fluorescent intensity and normalizing to the no-stimulation condition for each unique cell population and patient sample. Data are shown as mean $\pm$ SD. BL, baseline; W, week.

In conclusion, our results demonstrated that in the face of CD25 blockade, human FOXP3+ cells decline in number but retain the phenotypic and functional characteristics of the Treg lineage. In the context of a T cell–mediated autoimmune disease, the aggregate effect of long-term blockade of CD25-dependent IL-2 signaling is a reduction in autoimmune pathology and therapeutic benefit.

Disclosures

References

1. Josefowicz, S. Z., L.-F. Lu, and A. Y. Rudensky. 2012. Regulatory T cells: mechanisms of differentiation and function. *Annu. Rev. Immunol.* 30: 531–564.
2. Cheng, G., A. Yu, and T. R. Malek. 2011. T-cell tolerance and the multi-functional role of IL-2R signaling in T-regulatory cells. *Immunol. Rev.* 241: 63–76.
3. Wildin, R. S., F. Ramsdell, J. Peake, F. Faravelli, J. L. Casanova, N. Buist, E. Levy-Lahad, M. Mazzella, O. Goulet, L. Perroni, et al. 2001. X-linked neonatal diabetes mellitus, enteropathy and endocrinopathy syndrome is the human equivalent of mouse scurfy. *Nat. Genet.* 27: 18–20.
4. Bacchetta, R., L. Passerini, E. Gambineri, M. Dai, S. E. Allan, L. Perroni, F. Dagna-Bricarelli, C. Sartirana, S. Matthes-Martin, A. Lawitschka, et al. 2006. Defective regulatory and effector T cell functions in patients with *FOXP3* mutations. *J. Clin. Invest.* 116: 1713–1722.
5. Fontenot, J. D., M. A. Gavin, and A. Y. Rudensky. 2003. Foxp3 programs the development and function of CD4+CD25+ regulatory T cells. *Nat. Immunol.* 4: 330–336.

6. Hori, S., T. Nomura, and S. Sakaguchi. 2003. Control of regulatory T cell development by the transcription factor *Foxp3. Science* 299: 1057–1061.

7. Miyao, T., S. Floess, R. Setoguchi, H. Luche, H. J. Fehling, H. Waldmann, J. Huehn, and S. Hori. 2012. Plasticity of Foxp3(+) T cells reflects promiscuous Foxp3 expression in conventional T cells but not reprogramming of regulatory T cells. *Immunity* 36: 262–275.

8. Brusko, T. M., A. L. Putnam, and J. A. Bluestone. 2008. Human regulatory T cells: role in autoimmune disease and therapeutic opportunities. *Immunol. Rev.* 223: 371–390.

9. Zhou, X., S. L. Bailey-Bucktrout, L. T. Jeker, C. Penaranda, M. Martínez-Llordella, M. Ashby, M. Nakayama, W. Rosenthal, and J. A. Bluestone. 2009. Instability of the transcription factor Foxp3 leads to the generation of pathogenic memory T cells in vivo. *Nat. Immunol.* 10: 1000–1007.

10. McClymont, S. A., A. L. Putnam, M. R. Lee, J. H. Esensten, W. Liu, M. A. Hulme, U. Hoffmüller, U. Baron, S. Olek, J. A. Bluestone, and T. M. Brusko. 2011. Plasticity of human regulatory T cells in healthy subjects and patients with type 1 diabetes. *J. Immunol.* 186: 3918–3926.

11. Bailey-Bucktrout, S. L., M. Martinez-Llordella, X. Zhou, B. Anthony, W. Rosenthal, H. Luche, H. J. Fehling, and J. A. Bluestone. 2013. Self-antigen-driven activation induces instability of regulatory T cells during an inflammatory autoimmune response. *Immunity* 39: 949–962.

12. Malek, T. R. 2008. The biology of interleukin-2. *Annu. Rev. Immunol.* 26: 453–479.

13. Malek, T. R., and I. Castro. 2010. Interleukin-2 receptor signaling: at the interface between tolerance and immunity. *Immunity* 33: 153–165.

14. Waldmann, T. A. 2002. The IL-2/IL-15 receptor systems: targets for immunotherapy. *J. Clin. Immunol.* 22: 51–56.

15. Ota, K., M. Matsui, E. L. Milford, G. A. Mackin, H. L. Weiner, and D. A. Hafler. 1990. T-cell recognition of an immunodominant myelin basic protein epitope in multiple sclerosis. *Nature* 346: 183–187.

16. Wucherpfennig, K. W., K. Ota, N. Endo, J. G. Seidman, A. Rosenzweig, H. L. Weiner, and D. A. Hafler. 1990. Shared human T cell receptor V beta usage to immunodominant regions of myelin basic protein. *Science* 248: 1016–1019.

17. Allegretta, M., J. A. Nicklas, S. Sriram, and R. J. Albertini. 1990. T cells responsive to myelin basic protein in patients with multiple sclerosis. *Science* 247: 718–721.

18. Gold, R., G. Giovannoni, K. Selmaj, E. Havrdova, X. Montalban, E. W. Radue, D. Stefoski, R. Robinson, K. Riester, J. Rana, et al; SELECT study investigators. 2013. Daclizumab high-yield process in relapsing-remitting multiple sclerosis (SELECT): a randomised, double-blind, placebo-controlled trial. *Lancet* 381: 2167–2175.

19. Wiendl, H., and C. C. Gross. 2013. Modulation of IL-2Rα with daclizumab for treatment of multiple sclerosis. *Nat. Rev. Neurol.* 9: 394–404.

20. Bielekova, B., M. Catalfamo, S. Reichert-Scrivner, A. Packer, M. Cerna, T. A. Waldmann, H. McFarland, P. A. Henkart, and R. Martin. 2006. Regulatory CD56(bright) natural killer cells mediate immunomodulatory effects of IL-2Ralpha-targeted therapy (daclizumab) in multiple sclerosis. *Proc. Natl. Acad. Sci. USA* 103: 5941–5946.

21. Martin, J. F., J. S. Perry, N. R. Jakhete, X. Wang, and B. Bielekova. 2010. An IL-2 paradox: blocking CD25 on T cells induces IL-2-driven activation of CD56(bright) NK cells. *J. Immunol.* 185: 1311–1320.

22. Perry, J. S., S. Han, Q. Xu, M. L. Herman, L. B. Kennedy, G. Csako, and B. Bielekova. 2012. Inhibition of LTi cell development by CD25 blockade is associated with decreased intrathecal inflammation in multiple sclerosis. *Sci. Transl. Med.* 4: 145ra106.

23. Oh, U., G. Blevins, C. Griffith, N. Richert, D. Maric, C. R. Lee, H. McFarland, and S. Jacobson. 2009. Regulatory T cells are reduced during anti-CD25 antibody treatment of multiple sclerosis. *Arch. Neurol.* 66: 471–479.

24. Rech, A. J., R. Mick, S. Martin, A. Recio, N. A. Aqui, D. J. Powell, Jr., T. A. Colligon, J. A. Trosko, L. I. Leinbach, C. H. Pletcher, C. K. Tweed, A. DeMichele, K. R. Fox, S. M. Domchek, J. L. Riley, and R. H. Vonderheide. 2012. CD25 blockade depletes and selectively reprograms regulatory T cells in concert with immunotherapy in cancer patients. *Sci. Transl. Med.* 4: 134ra62.

25. Sehouli, J., C. Loddenkemper, T. Cornu, T. Schwachula, U. Hoffmüller, A. Grützkau, P. Lohneis, T. Dickhaus, J. Gröne, M. Kruschewski, et al. 2011. Epigenetic quantification of tumor-infiltrating T-lymphocytes. *Epigenetics* 6: 236–246.

26. Niemeyer, C. M., M. Adler, and R. Wacker. 2007. Detecting antigens by quantitative immuno-PCR. *Nat. Protoc.* 2: 1918–1930.

27. Miyara, M., Y. Yoshioka, A. Kitoh, T. Shima, K. Wing, A. Niwa, C. Parizot, C. Taflin, T. Heike, D. Valeyre, et al. 2009. Functional delineation and differentiation dynamics of human CD4+ T cells expressing the FoxP3 transcription factor. *Immunity* 30: 899–911.

28. Sakaguchi, S., D. A. Vignali, A. Y. Rudensky, R. E. Niec, and H. Waldmann. 2013. The plasticity and stability of regulatory T cells. *Nat. Rev. Immunol.* 13: 461–467.

29. da Silva Martins, M., and C. A. Piccirillo. 2012. Functional stability of Foxp3+ regulatory T cells. *Trends Mol. Med.* 18: 454–462.

30. Bailey-Bucktrout, S. L., and J. A. Bluestone. 2011. Regulatory T cells: stability revisited. *Trends Immunol.* 32: 301–306.

31. Baron, U., S. Floess, G. Wieczorek, K. Baumann, A. Grützkau, J. Dong, A. Thiel, T. J. Boeld, P. Hoffmann, M. Edinger, et al. 2007. DNA demethylation in the human *FOXP3* locus discriminates regulatory T cells from activated FOXP3(+) conventional T cells. *Eur. J. Immunol.* 37: 2378–2389.

32. Polansky, J. K., K. Kretschmer, J. Freyer, S. Floess, A. Garbe, U. Baron, S. Olek, A. Hamann, H. von Boehmer, and J. Huehn. 2008. DNA methylation controls *Foxp3* gene expression. *Eur. J. Immunol.* 38: 1654–1663.

33. Wieczorek, G., A. Asemissen, F. Model, I. Turbachova, S. Floess, V. Liebenberg, U. Baron, D. Stauch, K. Kotsch, J. Pratschke, et al. 2009. Quantitative DNA methylation analysis of *FOXP3* as a new method for counting regulatory T cells in peripheral blood and solid tissue. *Cancer Res.* 69: 599–608.

34. Yao, Z., Y. Kanno, M. Kerenyi, G. Stephens, L. Durant, W. T. Watford, A. Laurence, G. W. Robinson, E. M. Shevach, R. Moriggl, et al. 2007. Nonredundant roles for Stat5a/b in directly regulating *Foxp3. Blood* 109: 4368–4375.

35. Zorn, E., E. A. Nelson, M. Mohseni, F. Porcheray, H. Kim, D. Litsa, R. Bellucci, E. Raderschall, C. Canning, R. J. Soiffer, et al. 2006. IL-2 regulates *FOXP3* expression in human CD4+CD25+ regulatory T cells through a STAT-dependent mechanism and induces the expansion of these cells in vivo. *Blood* 108: 1571–1579.

36. Carbone, F., V. De Rosa, P. B. Carrieri, S. Montella, D. Bruzzese, A. Porcellini, C. Procaccini, A. La Cava, and G. Matarese. 2014. Regulatory T cell proliferative potential is impaired in human autoimmune disease. *Nat. Med.* 20: 69–74.

37. Viglietta, V., C. Baecher-Allan, H. L. Weiner, and D. A. Hafler. 2004. Loss of functional suppression by CD4+CD25+ regulatory T cells in patients with multiple sclerosis. *J. Exp. Med.* 199: 971–979.

38. Haas, J., A. Hug, A. Viehöver, B. Fritzsching, C. S. Falk, A. Filser, T. Vetter, L. Milkova, M. Korporal, B. Fritz, et al. 2005. Reduced suppressive effect of CD4+CD25high regulatory T cells on the T cell immune response against myelin oligodendrocyte glycoprotein in patients with multiple sclerosis. *Eur. J. Immunol.* 35: 3343–3352.

39. Kumar, M., N. Putzki, V. Limmroth, R. Remus, M. Lindemann, D. Knop, N. Mueller, C. Hardt, E. Kreuzfelder, and H. Grosse-Wilde. 2006. CD4+CD25+ FoxP3+ T lymphocytes fail to suppress myelin basic protein-induced proliferation in patients with multiple sclerosis. *J. Neuroimmunol.* 180: 178–184.

40. Schneider, A., S. A. Long, K. Cerosaletti, C. T. Ni, P. Samuels, M. Kita, and J. H. Buckner. 2013. In active relapsing-remitting multiple sclerosis, effector T cell resistance to adaptive Tregs involves IL-6–mediated signaling. *Sci. Transl. Med.* 5: 170ra15.

41. Kinnunen, T., N. Chamberlain, H. Morbach, T. Cantaert, M. Lynch, P. Preston-Hurlburt, K. C. Herold, D. A. Hafler, K. C. O'Connor, and E. Meffre. 2013. Specific peripheral B cell tolerance defects in patients with multiple sclerosis. *J. Clin. Invest.* 123: 2737–2741.

42. Venken, K., N. Hellings, R. Liblau, and P. Stinissen. 2010. Disturbed regulatory T cell homeostasis in multiple sclerosis. *Trends Mol. Med.* 16: 58–68.

43. Costantino, C. M., C. Baecher-Allan, and D. A. Hafler. 2008. Multiple sclerosis and regulatory T cells. *J. Clin. Immunol.* 28: 697–706.

44. Oldenhove, G., N. Bouladoux, E. A. Wohlfert, J. A. Hall, D. Chou, L. Dos Santos, S. O'Brien, R. Blank, E. Lamb, S. Natarajan, et al. 2009. Decrease of Foxp3+ Treg cell number and acquisition of effector cell phenotype during lethal infection. *Immunity* 31: 772–786.

45. Rubtsov, Y. P., R. E. Niec, S. Josefowicz, L. Li, J. Darce, D. Mathis, C. Benoist, and A. Y. Rudensky. 2010. Stability of the regulatory T cell lineage in vivo. *Science* 329: 1667–1671.

46. Komatsu, N., K. Okamoto, S. Sawa, T. Nakashima, M. Oh-hora, T. Kodama, S. Tanaka, J. A. Bluestone, and H. Takayanagi. 2014. Pathogenic conversion of Foxp3+ T cells into T_H17 cells in autoimmune arthritis. *Nat. Med.* 20: 62–68.

47. Zhang, Y., M. McClellan, L. Efros, D. Shi, B. Bielekova, M. T. Tang, V. Vexler, and J. P. Sheridan. 2014. Daclizumab reduces CD25 levels on T cells through monocyte-mediated trogocytosis. *Mult. Scler.* 20: 156–164.

48. Villarino, A. V., C. M. Tato, J. S. Stumhofer, Z. Yao, Y. K. Cui, L. Hennighausen, J. J. O'Shea, and C. A. Hunter. 2007. Helper T cell IL-2 production is limited by negative feedback and STAT-dependent cytokine signals. *J. Exp. Med.* 204: 65–71.

49. Jiang, W., N. R. Chai, D. Maric, and B. Bielekova. 2011. Unexpected role for granzyme K in CD56bright NK cell-mediated immunoregulation of multiple sclerosis. *J. Immunol.* 187: 781–790.

50. Li, Z., W. K. Lim, S. P. Mahesh, B. Liu, and R. B. Nussenblatt. 2005. Cutting edge: in vivo blockade of human IL-2 receptor induces expansion of CD56(bright) regulatory NK cells in patients with active uveitis. *J. Immunol.* 174: 5187–5191.